Journal of Fisheries
Volume 14 Issue 1 April 2026
Peer Reviewed | Open Access

eISSN 2311-3111
pISSN 2311-729X

DOI: https://doi.org/10.17017/j.fish.1193

Original Article

Modelling of 2,4-dichlorophenol, an emerging pollutant removal from water by adsorption onto sugarcane bagasse biochar using response surface methodology

Tapas Paul[1,2] • Rishika M S[1] • Bhautik D. Savaliya[1] • Saurav Kumar[1] • Pritam Sarkar[1] • Prasenjit Pal[1] • S.P. Shukla[1] • Kundan Kumar[1] • Ashish Kumar Jha[3] • Ganesh Kumar[4] • Supratim Malla[5]

[1] *ICAR-Central Institute of Fisheries Education, Mumbai - 400 061, Maharashtra, India*
[2] *College of Fisheries, Bihar Animal Sciences University, Kishanganj - 855107, Bihar, India*
[3] *ICAR-Central Institute of Fisheries Technology, Veraval - 362 265, Gujarat, India*
[4] *Rani Lakshmi Bai Central Agricultural University, Jhansi, Uttar Pradesh-284003, India*
[5] *College of Fisheries, Central Agricultural University, Agartala - 799 210, Tripura, India*

Correspondence
Saurav Kumar; ICAR-Central Institute of Fisheries Education, Mumbai - 400 061, Maharashtra, India
saurav@cife.edu.in and sauravsinha535@gmail.com

Manuscript history
Received 13 January 2026 | Accepted 10 February 2026 | Published online 18 February 2026

Citation
Paul T, Rishika MS, Savaliya BD, Kumar S, Sarkar P, Pal P, Shukla SP, Kumar K, Jha AK, Kumar G, Malla S (2026) Modelling of 2,4-dichlorophenol, an emerging pollutant removal from water by adsorption onto sugarcane bagasse biochar using response surface methodology. Journal of Fisheries 14(1): 141214. DOI: 10.17017/j.fish.1193

Abstract
This study evaluated the potential of sugarcane bagasse biochar as a low-cost adsorbent for removing 2, 4-dichlorophenol (2, 4-DCP), an emerging pollutant from water using adsorption modelling and response surface methodology. It aimed to determine optimal combinations of concentration, contact time, pH and dose for maximizing contaminant uptake in batch and column systems. Batch adsorption experiments were planned using a Box–Behnken response surface experimental design with initial 2, 4-DCP concentration (25, 50, and 75 mg L^{-1}), contact time (20, 40, and 60 min), solution pH (5, 7, and 9), and biochar dosage (6.25, 12.5, and 25 mg). Fixed-bed column studies were conducted under continuous flow to assess dynamic performance and breakthrough behaviour. Adsorption equilibrium, kinetics and column behaviour were analysed using standard isotherm and kinetic models, supported by surface and functional-group characterization. The optimized batch conditions produced removal efficiencies of about 95% with high monolayer adsorption capacity on a homogeneous biochar surface. The equilibrium data followed a monolayer adsorption model, while kinetic analysis indicated rapid uptake controlled primarily by surface-site availability. Column studies showed high dynamic capacity and well-defined breakthrough characteristics under the tested flow conditions. Sugarcane bagasse biochar proved to be an efficient and technically suitable material for removing phenolic contaminants such as 2, 4-DCP from water. The findings demonstrate a productive use of agro-industrial waste for water purification and support its application in practical treatment units for removing emerging pollutants in aquatic environments.

Keywords: 2, 4-dichlorophenol; adsorption; modelling; response surface methodology; sugarcane bagasse biochar

1 | INTRODUCTION

In recent times, emerging pollutants released from household products, pharmaceuticals, industrial activities, and agricultural practices have gained attention globally due to higher toxicity in aquatic environments (Kumar *et al.* 2024a, 2024b). These substances are increasingly detected in natural waters due to their continuous input, incomplete removal by conventional treatment systems, and environmental persistence. Among the various EPs, 2, 4-dichlorophenol (2, 4-DCP) is of relevance owing to its frequent occurrence and chemical reactivity in aquatic systems (Brausch and Rand 2011; Liu *et al.* 2025). It is formed both through environmental transformation processes, such as the photodegradation of triclosan, and through industrial production associated with herbicide manufacturing. Reported formation yields of 2, 4-DCP range between 3 and 12%, depending on prevailing conditions (Latch *et al.* 2005). The widespread detection of 2, 4-DCP in rivers, coastal waters, and stormwater systems highlights its growing environmental significance (Chiron *et al.* 2007; Liu *et al.* 2025).

Ecotoxicological studies have demonstrated that 2, 4-DCP exerts adverse effects across multiple trophic levels, affecting aquatic plants (Ensley *et al.* 1994), fish (Hu *et al.* 2021), molluscs (Xia *et al.* 2016), microalgae (Petroutsos *et al.* 2008), and microbial communities (Song *et al.* 2020). Median lethal concentration (LC_{50}) values indicate its potential to induce acute toxicity. In addition, chronic exposure has been associated with genotoxic, cytotoxic, neurotoxic, immunotoxic, biochemical, and haematological effects in exposed organisms (Celcey 2019; Hu *et al.* 2021; Imade *et al.* 2024). Owing to its persistence and ecological risks, the effective removal of 2, 4-DCP from aquatic systems has become a critical environmental priority. Although advanced treatment technologies such as ozonation, electrochemical oxidation, and chlorination have been explored, their application is often limited by high operational costs, energy demand, and infrastructural requirements (Wahyudi *et al.* 2020; Pan *et al.* 2021). Furthermore, chemical treatment of commonly used compounds such as triclosan can lead to the secondary formation of 2, 4-DCP, thereby exacerbating environmental contamination (Li *et al.* 2018). While bioremediation represents an environmentally benign alternative, its efficiency and scalability under field conditions remain challenging. Consequently, adsorption-based approaches using low-cost and sustainable materials have emerged as promising alternatives for the efficient removal of 2, 4-DCP, forming the basis of the present investigation. This technique is favored due to its simple operation, low energy requirements, and operational flexibility. Among various adsorbents, biochar has gained prominence owing to its high porosity, extensive surface area, and aromatic carbon structure, which collectively enhance its ability to capture organic contaminants (Rishika *et al.* 2024). Adsorption of organic pollutants onto biochar is primarily controlled by monolayer chemisorption, in addition to pore filling, hydrogen bonding, π–π interactions, and electrostatic forces (Ahmed *et al.* 2018; Czech *et al.* 2021; Tan *et al.* 2021; Dong *et al.* 2024) contribution to removal process. These properties make the biochar as an efficient and economical material for the remediation of 2, 4-DCP and related organic pollutants from wastewater.

In recent times various agro waste products has been utilized to produce biochar, among which sugarcane bagasse has gained extensive attention from the scientific community (Zafeer *et al.* 2024). In the current era of energy conservation, as both developed and developing nations shifting towards non-petroleum-based energy sources, the sugarcane-derived ethanol industry has emerged as a major focus of global interest. However, while doing so the industry produced solid waste with fixed carbon content known as sugarcane bagasse (Ghosh 2016). It has also been noted that improper disposal of bagasse can lead to significant environmental harm, adversely affecting both plant and animal life (Sharma *et al.* 2024). In this context, utilizing sugarcane bagasse for the removal of emerging pollutants offers a dual advantage, enabling effective management of waste generated by the ethanol industry while supporting environmentally sustainable pollutant remediation. Its benefits include wide availability, high production yield, ease of collection, relatively stable composition, and consistent physicochemical properties. In addition, previously available literature also proved that biochar produced from sugarcane bagasse effectively remove various organic and inorganic pollutants from the aquatic system (Tahir *et al.* 2016; Prasannamedha *et al.* 2022; Rishika *et al.* 2024; Ponnuchamy *et al.* 2025). Keeping this in prelude, the present investigation aims to remove 2, 4-DCP, an emerging pollutant removal from water by adsorption onto sugarcane bagasse biochar using response surface methodology.

2 | METHODOLOGY

2.1 Preparation of biochar

Sugarcane bagasse (SB) was sourced from a local juice vendor in Mumbai, India, and thoroughly washed with deionized water to remove adhering surface impurities prior to further processing. After being sun-dried for around three days to eliminate moisture, the sugarcane bagasse was pyrolyzed at 400°C temperature in a biochar kiln under oxygen-limited conditions with a holding time of 15 minutes.

2.2 Batch experiments for 2, 4-DCP removal

A statistical optimization approach combining Response Surface Methodology (RSM) with a Box–Behnken Design (BBD) was applied to evaluate the batch adsorption performance of pyrolyzed sugarcane bagasse biochar (SBB)

for the removal of 2, 4-DCP. This approach was used to assess and optimize the influence of key operational parameters, including initial 2, 4-DCP concentration, contact time, solution pH, and biochar dosage—on adsorption efficiency. The total number of experimental runs required for model development and optimization was calculated using the following expression (Box and Behnken 1960):

$$N = 2k(k-1) + Cp$$

where N denotes the total number of experimental trials, k corresponds to the number of independent variables, and C_p represents the number of centre points included in the design. A Box–Behnken experimental matrix comprising four factors at three coded levels was adopted, resulting in a total of 29 experimental runs. The selected independent variables included initial 2, 4-dichlorophenol (2, 4-DCP) concentration (A: 25, 50, and 75 mg L^{-1}), contact time (B: 20, 40, and 60 min), solution pH (C: 5, 7, and 9), and biochar dosage (D: 6.25, 12.5, and 25 mg).

Batch adsorption experiments were performed using 10 mL aliquots of 2, 4-DCP solution, with an adsorbent mass of 15.625 mg added to each flask. The reaction mixtures were agitated at 150 rpm using a temperature-regulated orbital shaker (Rotek LSV, India), while maintaining the temperature within the range of 25–27°C. Upon completion of the adsorption period, solid–liquid separation was achieved by filtration through glass microfiber filter papers (Whatman, USA) to obtain clarified samples for analysis. Kinetic adsorption studies were subsequently conducted using sugarcane bagasse biochar pyrolyzed at 400°C (SBB-400), evaluating the effects of varying solute concentrations (25–75 mg L^{-1}), contact durations (20–60 min), pH conditions (5–9), and adsorbent dosages (6.25–25 mg per 10 mL solution). All experiments were carried out under controlled laboratory conditions at 27±1°C. For each experimental run, the conical flasks were loosely sealed with cotton plugs and placed on a bench-top orbital shaker operating at 150 rpm. At predetermined intervals, a 5 mL sample was withdrawn and filtered through Whatman No. 1 filter paper to remove suspended biochar particles. The residual concentration of 2, 4-DCP in samples corresponding to optimized conditions was quantified using reverse-phase high-performance liquid chromatography (RP-HPLC) equipped with an iUHPLC-3000PLUS system (Analytical Technologies Limited, India). The analytical conditions followed were mobile phase as acetonitrile: water: orthophosphoric acid (800:200:1), pump rate 1.8 mL min^{-1}, injection volume 5µL, column temperature 25°C, detector wavelength 225 nm and retention time 2.2–2.3 min.

2.3 Adsorption isotherm modelling

2.3.1 Langmuir isotherm: The linearized Langmuir isotherm model (Langmuir 1918) was fitted to the 2, 4-DCP adsorption data at different doses. This model is described as:

$$\frac{C_e}{q_e} = \frac{1}{q_m b} + \frac{C_e}{q_m}$$

where b is the Langmuir affinity constant, q_m represents the maximum sorption capacity, C_e denotes the equilibrium concentration, and q_e corresponds to the amount adsorbed at equilibrium. The fundamental characteristics of the Langmuir isotherm were further evaluated using the dimensionless separation factor (RL), expressed as follows (Hall *et al.* 1966).

$$R_L = \frac{1}{1 + bC_o}$$

Where, b represents the Langmuir constant and C_o denotes the initial solute concentration. The nature of the adsorption process can be interpreted from the value of the separation factor (RL): adsorption is considered favourable when $0 < RL < 1$, unfavourable when $RL > 1$, and linear when $RL = 1$.

2.3.2 Freundlich isotherm: The Freundlich isotherm describes multilayer adsorption on heterogeneous surfaces (Freundlich 1906) and is expressed as:

$$\log q_e = \log K_F + \frac{1}{n} \log C_e$$

where C_e is the equilibrium concentration, K_F is the biosorption capacity, q_e is the equilibrium adsorption capacity, and n is the sorption's deviation from linearity.

2.4 Adsorption kinetic modelling

Pseudo first-order (PFO) and pseudo second order (PSO) were used to ascertain 2, 4-DCP adsorption process (Ho *et al.* 2000).

2.4.1 Pseudo first-order (PFO) and Pseudo second order (PSO) model: After fitting the adsorption kinetic data to the pseudo-first-order model, the predicted equilibrium adsorption capacities at different 2, 4-DCP concentrations were compared with the experimental values. The linearized form of the PFO model is:

$$\log(q_e - q_t) = \log q_e - \left(K_1 \times \frac{t}{2.303}\right)$$

Experimental removal and adsorption of 2, 4-DCP at varying doses were compared with the calculated equilibrium capacities. The adsorption kinetics were modelled using the pseudo-second-order equation, linearized as follows:

$$\frac{t}{q_t} = \frac{1}{K_2 q_e^2} + \frac{1}{q_e}$$

where q_t is the adsorption capacity at time t, q_e is the equilibrium adsorption capacity, and K_1 and K_2 are respective rate constants.

2.5 Removal efficiency

The 2, 4-DCP removal efficiency of the column bed was

determined at different time intervals using the following equation (Amin *et al*. 2016):

$$\text{Removal efficiency (\%)} = (C_0 - C_e) / I_0 \times 100$$

Where C_o and C_e denote the 2, 4-DCP concentrations before and after treatment, respectively.

2.6 Adsorption capacity

Adsorption capacity for 2, 4-DCP was determined as the total amount adsorbed per unit dry biomass (M) in the column. It is calculated using the equation:

$$\text{Adsorption capacity (mg g}^{-1}) = \frac{\Sigma[(C_o - C_i) \times V_i]}{M}$$

C_o is the initial 2, 4-DCP concentration, C_i the concentration in the *i*th effluent fraction, and V_i its collected volume.

2.7 Breakthrough point

The ratio of 2, 4-DCP influent concentration (C_0) to effluent concentration (C_i) was used to identify the breakthrough point. A ratio of 1.0 to 1.05 marked the breakthrough point.

2.8 Column bed adsorption and its modelling

2.8.1 Thomas model: The Thomas model characterizes adsorption in a continuous-flow fixed-bed (Figure 1) system by assuming that 2, 4-DCP is transported from the bulk solution to the adsorbent surface through a liquid film, where the overall adsorption rate is governed primarily by mass transfer at the solid–liquid interface rather than by chemical reaction kinetics (Thomas 1944). The linearized form of the Thomas model for such a system is given as:

$$\ln (C_0/C_t - 1) = K_{th}\, q_{max}\, m / Q - K_{th} C_0 t$$

where, C_o is the initial 2, 4-DCP concentration (mg L^{-1}), C_t is the effluent concentration at time *t* (mg L^{-1}), q_{max} is the maximum adsorption capacity (mg g^{-1}), Q is the flow rate (mL min^{-1}), m is the adsorbent mass in the column (g), t is time (min), and K_{th} is the Thomas rate constant (mL mg^{-1} min^{-1}). The parameters K_{th} and q_{max} were determined from the slope and intercept of the linear plot of ln ($C_o/C_t - 1$) versus t. The experimental maximum adsorption capacity was calculated at the exhaustion point, defined as t_e or when $C_t/C_o = 0.5$.

2.8.2 Yoon- nelson model: The Yoon–Nelson model assumes that the rate of decrease in the probability of adsorption for each solute molecule governs both the adsorption process and the breakthrough behaviour in a fixed-bed system (Yoon and Nelson, 1984). The model can be expressed in its linearized form as:

$$\ln\left(\frac{C_t}{C_o - C_t}\right) = K_{yn} t - K_{yn} \tau$$

C_t represents the effluent 2, 4-DCP concentration at time *t* (mg L^{-1}), C_o is the initial concentration (mg L^{-1}), τ is the time required for 50% breakthrough (min), t is time (min), and K_{yn} is the Yoon–Nelson rate constant (min^{-1}). The parameters K_{yn} and τ were determined from the slope and intercept of the linear plot of ln (C_t / (C_o − C_t)) versus t. According to this model, the total amount of 2, 4-DCP adsorbed in the column corresponds to half of the cumulative influent passing through the bed within a period of 2τ. The maximum adsorption capacity can then be calculated using the following equation:

$$q_{max} = \frac{\frac{1}{2} C_o \frac{Q}{1000}\, 2\tau}{m}$$

Where, Q is the flow rate (mL min^{-1}), C_o is the initial 2, 4-DCP concentration (mg L^{-1}), and m is the total mass of adsorbent in the column (g).

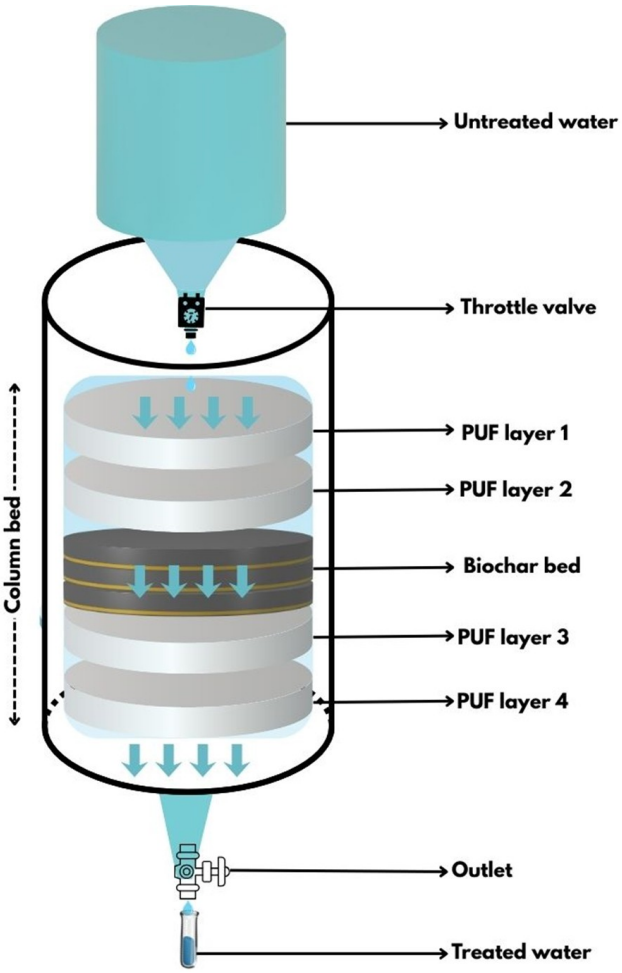

FIGURE 1 Design of polyurethane foam based fixed bed column filtration unit for removal of 2, 4-dichlorophenol.

2.9 Data analysis

The batch study experimental data were processed using Design-Expert software, with analysis of variance (ANOVA) employed to assess the significance of the fitted linear model. Three-dimensional (3D) response surface plots were generated to visualize the interactions among the independent variables. For the column study, 2, 4-DCP removal data were subjected to one-way ANOVA using IBM SPSS Statistics version 22.0. All results are expressed

as mean ± standard error (SE). Comparisons among treatment means were conducted using Duncan's Multiple Range Test (DMRT), with statistical significance defined at $p < 0.05$.

3 | RESULTS AND DISCUSSION

3.1 Batch adsorption optimization

Response surface methodology and Box–Behnken design using initial concentration (A) 25, 50, 75 mg L^{-1}, contact time (B) 20, 40, 60 min, pH (C) 5, 7, 9, and adsorbent dose (D) 6.25, 15.63, 25 mg showed removal efficiencies across the experimental design ranging from 33.6 to 94.9% (Figure 2). The quadratic model was found to be significant (ANOVA: $F = 4.47$, $p = 0.004$). Among the linear factors, contact time significantly improved removal (ANOVA: $F = 11.93$, $p = 0.003$). The elimination was also significantly impacted by the quadratic factors A^2 ($p = 0.006$) and C^2 ($p < 0.001$), suggesting non-linear effects of pH and starting concentration. The final regression model was the coefficient of determination ($R^2 = 0.81$) showed that the model could explain ~81% of variability. Adjusted R^2 was 0.6342, while the adequate precision value of 7.27 (>4) indicated a good signal-to-noise ratio. The optimization of 2, 4-DCP removal using SBB showed that the adsorption was significantly influenced by the initial concentration, contact time, pH, and the dose of adsorbent. At lower concentrations 25 mg L^{-1}, due to the occurrence of abundant binding sites highest percentage of adsorption was achieved. Similar results were observed by Matolia *et al.* (2019) and Rishika *et al.* (2024) for removal of TCS from water by adsorption process.

3.2 Effect of independent variables

The removal efficiency was very high about 90% at the lowest concentration of 25 mg L^{-1}, due to availability of active binding sites on the biochar surface in relation to adsorbate molecules. At the concentration of 50 mg L^{-1}, rate of removal increased further and reached a maximum of 94.9% which indicates that moderate concentration gives the favourable driving forces. At the highest concentration of 75 mg L^{-1}, 70–80% removal rate was achieved this decrease is due to adsorbent saturation and limited binding sites. The contact time plays very crucial role in removal at the contact time of 20 mins, relatively low removal rate of about 60–70% was observed, improved adsorption of about 85–90% achieved with contact time of 40 mins. While maximum efficiency achieved near 60 mins, about 94–95% removal in consistent with pseudo second-order kinetics. At acidic pH of 5, moderate removal rate was achieved (75–80%), as excess protons competed with the 2, 4-DCP molecules. The removal peaked (94–95%) at near neutral pH indicating optimal electrostatic interaction and hydrogen bonding between surface functional groups of biochar and 2, 4-DCP. At alkaline pH (9), efficiency declined (70–75%), due to increased deprotonation of 2, 4-DCP and enhanced electrostatic repulsion from negatively charged biochar surfaces. At the low adsorbent dose (6.25 mg), removal was limited (60–70%), owing to fewer available adsorption sites. Increasing dose to 12.5 mg enhanced removal (85–90%), while further increase to 25 mg only slightly improved removal (92–94%), showing diminishing returns once sufficient binding sites were available.

The equilibrium was achieved within 60 mins as consequence of contact time-dependent increase in removal up to 60 mins which is in accordance with Sun *et al.* (2017) for phenolic pollutants. pH also played a crucial role as adsorption was optimal near neutrality (pH 6.7–7), since 2, 4-DCP exists in its molecular form and the SBB surface carries weak negative charge, favouring π–π interactions and hydrogen bonding. At low pH, competition with protons reduced removal, whereas at high pH, deprotonation of both surface and solute led to electrostatic repulsion (Wu *et al.* 2019; Rishika *et al.* 2024).

3.3 Optimization and validation

Optimization through numbers based on desirability function suggested the best operating conditions: initial concentration 50 mg L^{-1}, contact time 50–55 mins, pH 6.7-7, and dose 13-15 mg. Under these conditions, the predicted removal efficiency was 94.9–95.0%. Multiple solutions confirmed robustness, all giving removal above 94.9% with desirability = 1. The analysis revealed that contact time and pH were the most influential parameters. Sufficient contact time ensured maximum interaction with biochar surface, while near-neutral pH provided favourable electrostatic and π–π interactions. Extremely low or high concentrations and doses caused efficiency losses due to either low driving force (low concentration), site saturation (high concentration), or redundant surface area (excess dose). The optimum dose of 13–15 mg yielded near-complete removal (~95%) without excessive surface redundancy is consistent with Amin *et al.* (2016). Overall, the RSM–BBD optimization established that moderate concentration, neutral pH, and adequate contact time ensure maximum utilization of available active sites on SBB.

3.4 Adsorption isotherm studies for 2, 4-DCP

Langmuir and Freundlich isotherms were used to characterize the adsorption mechanism and surface behaviour of the adsorbent and to obtain 2, 4-DCP equilibrium data (Figure 3). The excellent fit to the data was provided by Langmuir model, which shows the monolayer adsorption of adsorbent on biochar surface with identical and energetically equivalent active binding sites with a correlation coefficient (R^2) of 0.972. The Langmuir constant (b) and the maximum monolayer adsorption capacity (q_{max}) were found to be 1.34 L mg^{-1} and 78.34 mg g^{-1}, respectively. The strong affinity between the 2, 4-DCP molecules and

the biochar surface reflected by high 'b' value. The favourable nature of adsorption was confirmed by the separation factor (*R*) values between 0.15 and 0.35. The fit of linearity of the Langmuir indicates that chemisorption is the dominant mechanism and adsorption is predominantly monolayer.

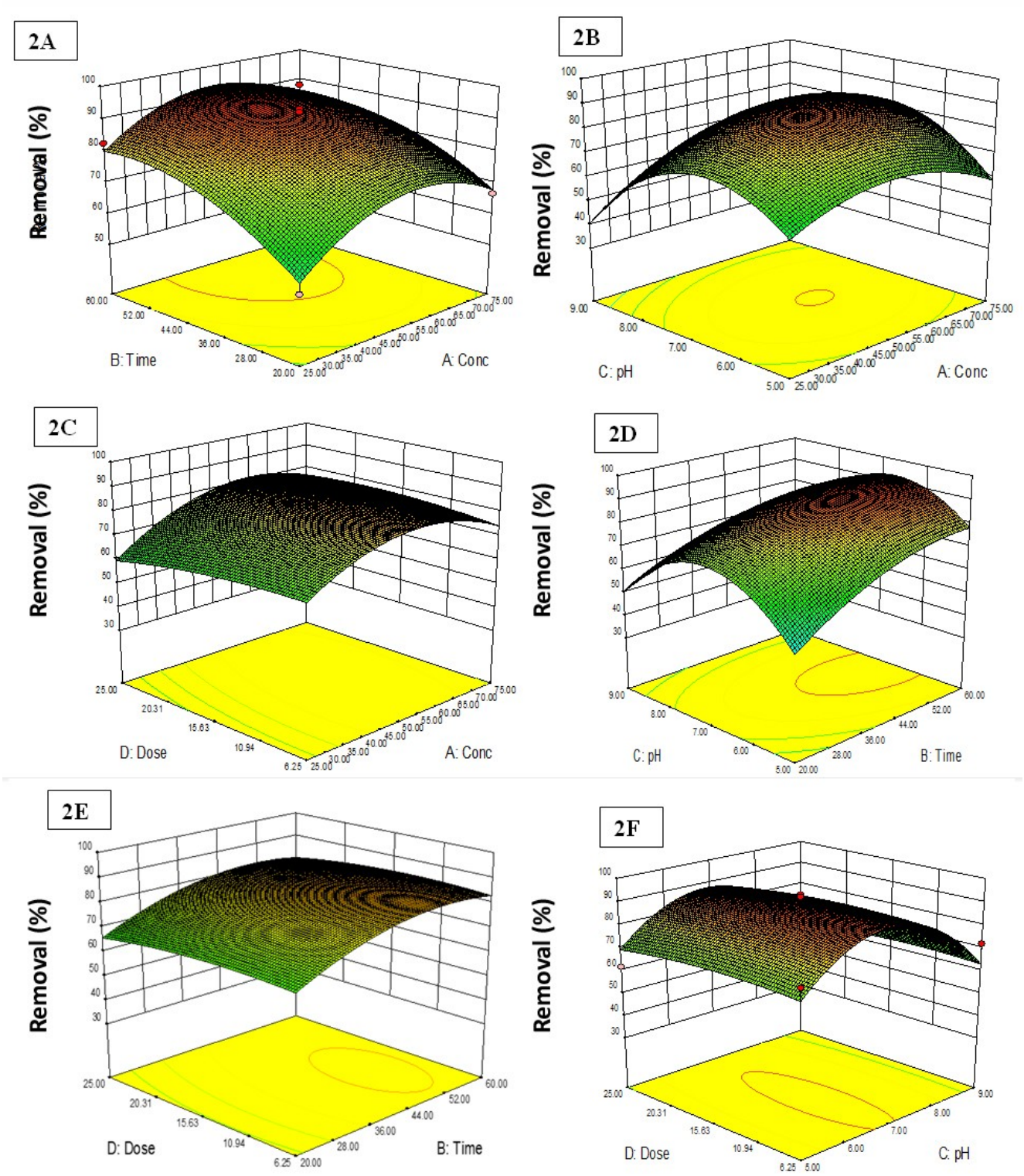

FIGURE 2 The interactive effect of (A) initial concentration and contact time, (B) initial concentration and pH, (C) initial concentration and adsorbent dose, (D) contact time and pH, (E) contact time and adsorbent dose, (F) pH and adsorbent dose on the removal efficiency of 2, 4-dichlorophenol.

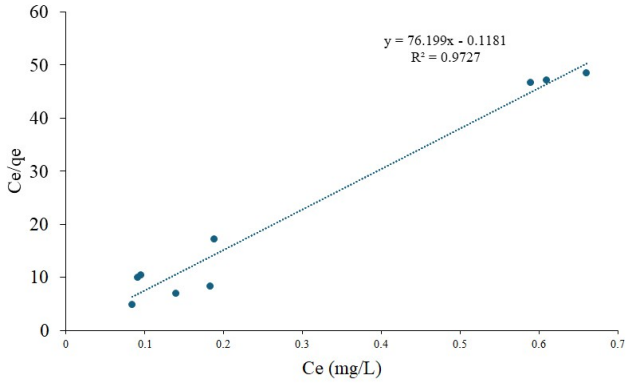

FIGURE 3 2, 4-dichlorophenol adsorption isotherm data fitted to Langmuir Isotherm. Data is presented in mean ± SE.

In contrast, the Freundlich model exhibited a very poor correlation (R^2 = 0.097), with calculated constants K_F = 54.48 (mg g^{-1}) (L $mg^{-1})^{1/n}$ and n = 0.93 (Table S1). Although the value of indicates a favourable adsorption process, the low regression coefficient implies that the Freundlich model does not adequately describe the adsorption behaviour of 2, 4-DCP onto biochar. These results confirm Langmuir-type monolayer adsorption of 2, 4-DCP on the adsorbent surface.

The data of equilibrium adsorption well fitted with the Langmuir model (R^2= 0.97), indicating the adsorption of 2, 4-DCP on homogeneous active binding sites are of monolayer. The maximum monolayer capacity (q_{max} = 78.34 mg g^{-1}) and high Langmuir constant (b = 1.34 Lmg^{-1}) indicate strong binding affinity and chemisorptive interactions between 2, 4-DCP molecules and biochar. The RL values (0.15–0.35) signify a favourable adsorption process (Hall *et al.* 1966). In the similar way the data was poorly fitted to Freundlich model (R^2= 0.097) suggests that multilayer adsorption on heterogeneous sites is less likely in this system. The uniform distribution of oxygenated functional groups (–OH, –COOH) on the biochar surface generated during pyrolysis leads to monolayer adsorption rather than the multilayer. Similar Langmuir-dominated behaviour for chlorinated phenols on carbonaceous materials has been reported by Tran *et al.* (2023) and Li *et al.* (2020). Thus, the isotherm results confirm that adsorption proceeds primarily through monolayer coverage dominated by π–π electron donor acceptor interactions and hydrogen bonding between 2, 4-DCP aromatic rings and biochar carbonaceous surface.

3.5 Adsorption kinetic modelling

To elucidate the rate-controlling mechanism, the adsorption kinetics of 2, 4-DCP onto biochar were evaluated using pseudo-first-order (PFO) and pseudo-second-order (PSO) kinetic models. The linearized PFO model, ln (q_e – q_t) = ln q_e – k_1t, produced an excellent linear fit with a correlation coefficient of R^2 = 0.99 and a rate constant k_1 = 0.0771 min^{-1}. This very high R^2 indicates that the PFO model accurately captures the time-dependent uptake behaviour, particularly during the initial and intermediate adsorption stages, and suggests that the rate is strongly governed by the availability of vacant surface sites and surface diffusion processes (Figure 4). The PSO model, also correlated well with the experimental data (R^2 ≈ 0.93, k_2 = 6.4×10^{-5} mg^{-1} min^{-1}) indicating that chemical sorption contributes to the overall mechanism however, the superior fit of the PFO model (R^2 = 0.99) implies that the adsorption kinetics are dominated by processes consistent with first-order behaviour under the studied conditions. Together, these results suggest a mixed mechanism in which rapid physical uptake and site availability control the early rate while chemisorption may become more influential as equilibrium is approached.

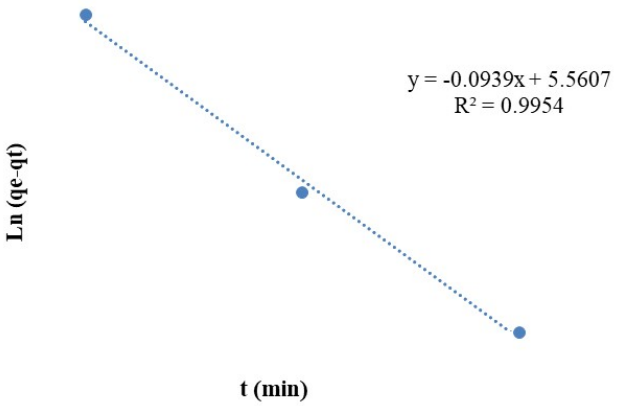

FIGURE 4 Pseudo first order model fitted 2, 4-dichlorophenol data at different concentration. Data are presented in Mean ± S.E, n = 3.

The adsorption kinetics followed the model of pseudo-first order likely (R^2 = 0.99) in comparison to the pseudo-second order model (Figure 5), which implies the rate of adsorption of 2, 4-DCP is largely attributed by the number of available binding sites and external mass transfer. The PSO dominance is characteristic of systems where physical sorption and diffusion through pores play the main role during early adsorption stages (Ho *et al.* 2000). This indicates that chemical interactions through hydrogen bonding or π–π stacking also contribute to the overall mechanism. The studies of phenolic pollutant adsorption on biochar and activated carbon, similar results were observed (Moussavi and Khosravi 2011). The quick diffusion of 2, 4-DCP molecules to the SBB surface and the gradual saturation of adsorption sites depicts the adsorption is rapid in the initial followed the equilibrium plateau. This in line with the intra-diffusion model given by Weber and Morris (1963), where surface adsorption dominates the initial phase followed by slower pore diffusion.

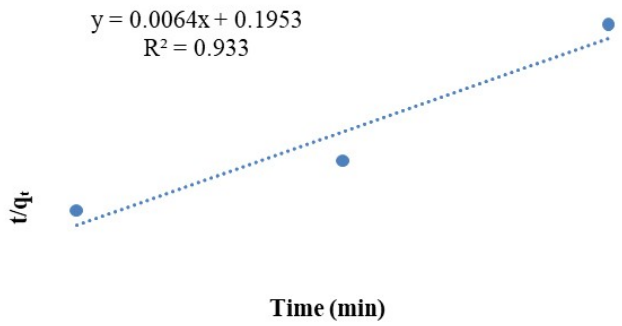

FIGURE 5 Pseudo second order model fitted 2, 4-dichlorophenol data at different concentration. Data are presented in Mean ± S.E, *n* = 3.

3.6 Scanning electron microscopy (SEM)

The surface of sugarcane bagasse biochar is a highly porous, with presence of well-defined fibrous structure and contains numerous open channels (Figure 6). The grooves and pores are clearly visible a large surface area available for adsorption. The presence of interactive functional surfaces was indicated by relatively smooth walls. The surface shows the deposition of adsorbate molecules, clogged pores, and partial coverage of fibrous network. The diffusion of 2, 4-DCP molecules into the porous matrix was observed in filled or blocked pores. The increase in the surface roughness, and irregular patches are typical signs of adsorbate accumulation. The biochar's porous and interconnected fibrous channels were clearly seen in SEM micrographs. The pore size reduction and rough texture appearance is indicative of surface coverage and molecular interaction between adsorbate and adsorbent (Chen *et al.* 2020). This kind of transformations is common in phenolic compounds adsorption, where the diffusion of small molecules into the micro- and mesoporous network causes blockage (Gopinath *et al.* 2021). The presence of heterogeneous surface topography after adsorption also suggests that multilayer interaction may occur locally, even though Langmuir fitting indicates dominant monolayer adsorption on average. These findings align with elemental mapping and FTIR results reported in related studies, showing that adsorption is often facilitated by aromatic ring interactions and the formation of weak chemical bonds (Li *et al.* 2020; Tran *et al.* 2023).

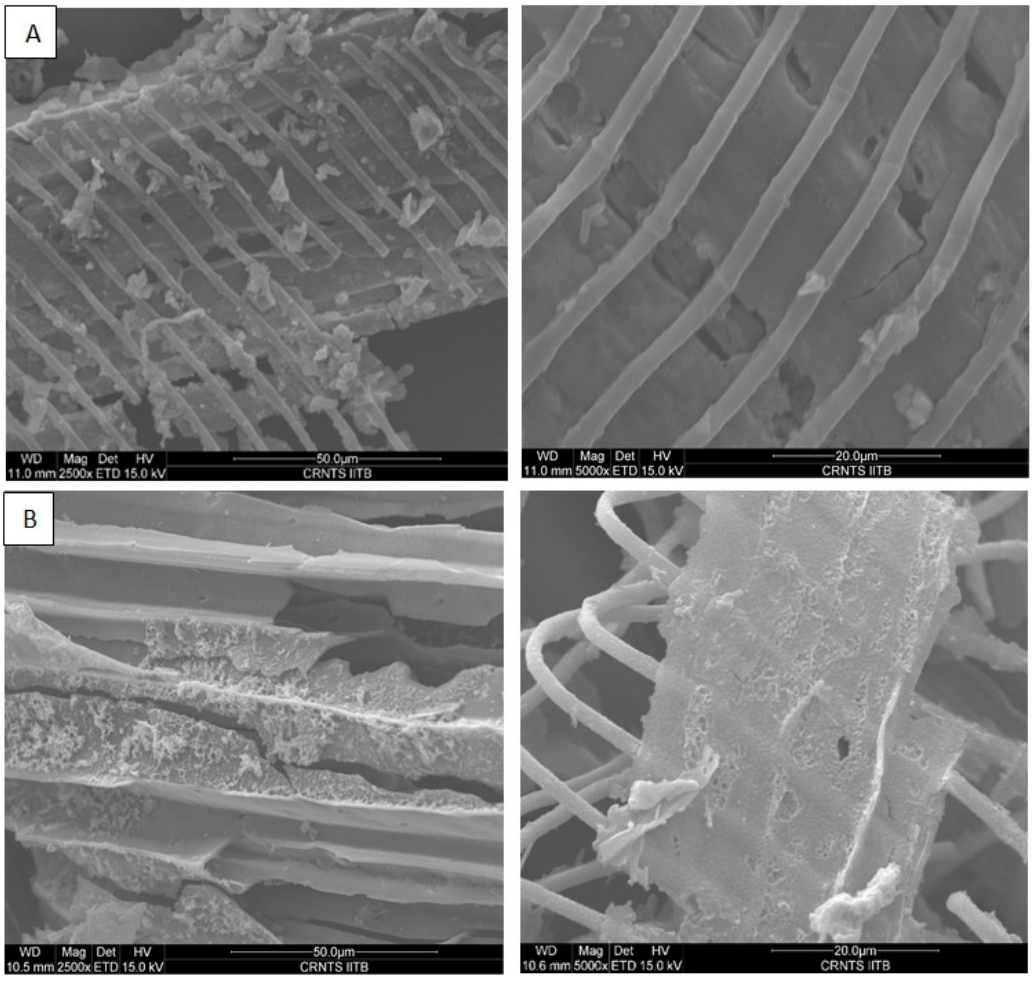

FIGURE 6 Scanning electron microscopy micrographs of sugarcane bagasse biochar before adsorption and after adsorption of 2, 4-dichlorophenol at magnifications (a) 2500X and (b) 5000X, showing well-defined porous structures and open channels.

3.7 Fourier transform infrared spectroscopy

The adsorption of 2, 4-DCP onto the biochar surface was analyzed using Fourier Transform Infrared (FTIR) spectroscopy, which revealed distinct spectral differences, confirming interactions with specific functional groups (Figure 7). The broad band observed around 3400–3450 cm^{-1} corresponds to the stretching vibrations of surface –OH groups, including hydroxyls and adsorbed water (Tran *et al.* 2023). Following adsorption, this band showed a slight reduction in intensity and a marginal shift toward lower wave numbers, suggesting hydrogen bonding between the phenolic –OH of 2, 4-DCP and the biochar's hydroxyl functionalities (Rishika *et al.* 2024). The C–H stretching vibrations of aliphatic $–CH_2$ and $–CH_3$ groups appeared at 2920–2850 cm^{-1}; remained unchanged, indicating that the aliphatic structures of the carbon matrix were unaffected. Conversely, the fingerprint region for C=C stretching of aromatic rings and conjugated carbonyl groups (1600–1620 cm^{-1}) became sharper and shifted slightly, pointing to π–π electron donor–acceptor interactions (Li *et al.* 2020). Additionally, the intensity of the aromatic C=C bending vibration peak increased at 1420–1450 cm^{-1}, confirming the presence of aromatic chlorophenolic compounds. A new or significantly enhanced band appeared at 1250–1300 cm^{-1} in the treated biochar, assigned to phenolic C–O stretching and C–Cl deformation modes typical of chlorophenol adsorption (Wu *et al.* 2019; Chen *et al.* 2020). Furthermore, a band at 1050–1080 cm^{-1} corresponding to C–O–C stretching vibrations suggested possible chemical associations with ether linkages. (Ho *et al.* 2000; Rishika *et al.* 2024). These spectral patterns confirm that π–π stacking, hydrogen bonding, and van der Waals interactions are the dominant adsorption mechanisms, further supported by the slight reduction in overall –OH and aromatic peak intensities.

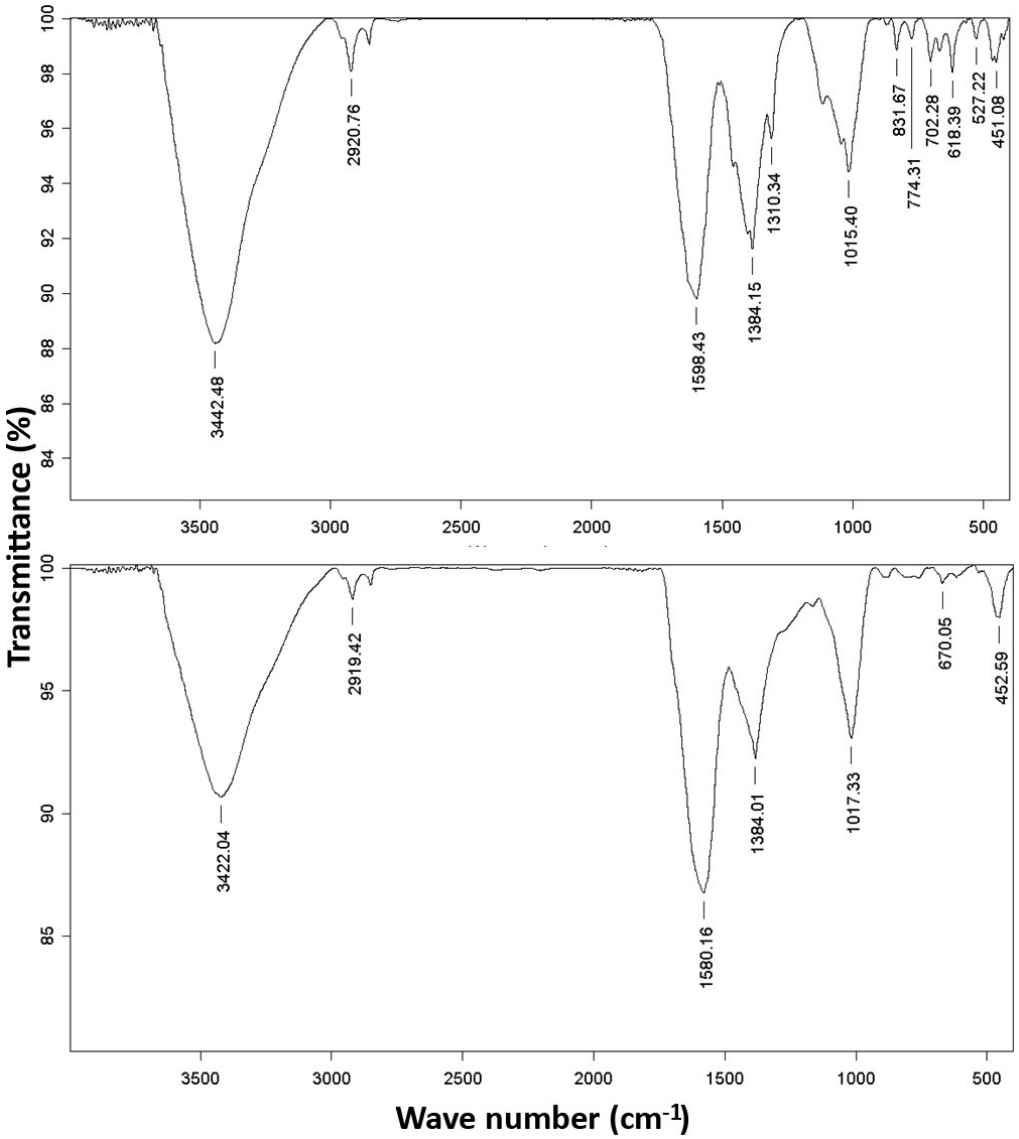

FIGURE 7 Fourier Transform Infrared spectroscopy micrographs showing control and after adsorption of 2, 4-dichlorophenol on to the surface of biochar.

3.8 Column adsorption and modelling

3.8.1 Thomas model: The Thomas and Yoon-Nelson models were employed to assess the column adsorption behaviour of 2, 4-DCP onto biochar to characterize the breakthrough performance and adsorption kinetics under dynamic flow circumstances (Figure 8). Thomas model was applied to relate solute concentration to time during fixed-bed column operation, assuming Langmuir-type adsorption and negligible axial dispersion. The linearized Thomas equation, exhibited excellent linearity with a correlation coefficient of R^2 = 0.98, confirming its suitability for modelling the column data. The estimated Thomas rate constant (k_{Th}) and maximum solid-phase adsorption capacity ($q_{max(cal)}$) were 0.0024 mL min^{-1} mg^{-1} and 100 mg g^{-1}, respectively (Table S2). The strong correlation indicates that the Thomas model successfully describes the mass transfer dynamics of 2, 4-DCP within the column and that the process is largely governed by external film diffusion and chemical interaction between the solute and the active sites of the biochar. The close agreement between the experimental capacity ($q_{max(exp)}$ = 78.3 mg g^{-1}) and the model-calculated value ($q_{max(cal)}$ = 100 mg g^{-1}) further supports the accuracy of this model in predicting adsorption performance. The provided excellent Thomas fit of R^2 = 0.98, depicts that the process of adsorption in the fixed bed column follows the Langmuir kinetics and is primarily attributed to mass transfer at the solid- liquid interface rather than by chemical reaction. The obtained Kth 0.0024 mL mg^{-1} min^{-1} and q_{max} values of 100 mg g^{-1} suggest strong binding affinity and efficient utilization of available binding sites in accordance with Chatterjee *et al.* (2011) and Amin *et al.* (2016). These results highlight that the dynamic adsorption system operates under favourable flow and contact conditions.

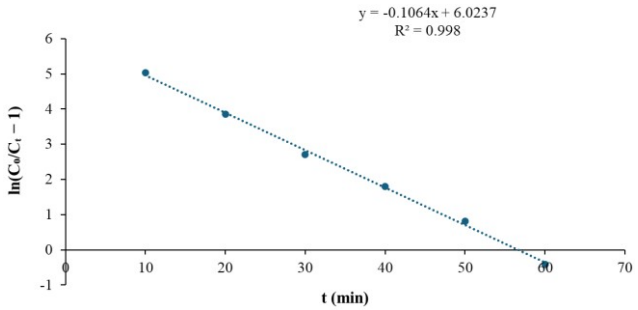

FIGURE 8 Thomas plot for 2, 4-dichlorophenol adsorption on column bed.

3.8.2 Yoon-Nelson model

The Yoon–Nelson model, which assumes that the probability of adsorption decreases exponentially with time, was used to describe the breakthrough curve without requiring detailed bed characteristics (Figure 9). The linearized equation has given the R^2 = 0.98, an excellent fit that indicated strong correlation between the experimental and theoretical predictions. The Yoon–Nelson rate constant (K_{yn}) and breakthrough time (τ) were calculated as 0.12 min^{-1} and 52.0 min, respectively. The τ value closely matched the experimentally observed breakthrough time, indicating that approximately 50% of 2, 4-DCP molecules exited the column at around 52 minutes of operation. The good correlation further suggests that the column adsorption process follows predictable kinetics and favourable breakthrough behaviour.

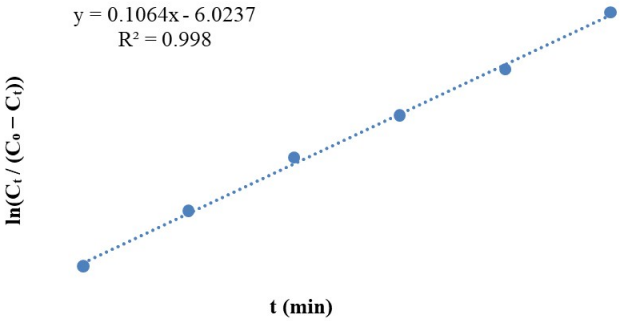

FIGURE 9 Yoon- Nelson plot for 2, 4-dichlorophenol adsorption on column bed.

Additionally, the Yoon–Nelson model exhibited a strong correlation (R^2 = 0.98) with the experimental data, yielding a rate constant (K_{yn} = 0.12 min^{-1}) and a breakthrough time (τ) of 52 min (Table S3). The close agreement between the observed and predicted τ values indicates that approximately 50% of the influent concentration was adsorbed by this time, which aligns with the experimental breakthrough profile. The model's prediction of an exponential decrease in adsorption probability confirms the progressive saturation of adsorption sites, with equilibrium reached near the predicted τ (Yoon and Nelson 1984). These findings are consistent with previous reports on phenolic pollutant removal in biochar-packed columns (Mohammadi *et al.* 2019). Collectively, the Thomas and Yoon–Nelson models demonstrate that 2, 4-DCP adsorption in a continuous column is highly efficient and predictable, following Langmuir-type monolayer dynamics under steady flow conditions.

4 | CONCLUSIONS

Response surface methodology optimized adsorption parameters, achieving about 95% 2, 4-DCP removal at moderate concentration, near-neutral pH, adequate contact time, and optimized biochar dose. Adsorption equilibrium followed the Langmuir isotherm with high monolayer capacity, indicating homogeneous surface binding. Fixed-bed column studies demonstrated high dynamic adsorption capacity with excellent fit to Thomas and Yoon–Nelson models, indicating predictable breakthrough performance. The excellent efficiency of removal of 2, 4-DCP in both batch and the column studies of sugarcane bagasse biochar reflects its porosity, high surface area, and functionalized matrix. The present study will

also act as baseline information for removal of such other emerging pollutants from water using low-cost adsorption technology. Future studies can be focused on utilising the modified biochar through chemical or mechanical activation for removal of 2, 4-DCP from aquatic environment.

ACKNOWLEDGEMENTS

The authors express heartfelt thanks to the Director & Vice Chancellor, ICAR-Central Institute of Fisheries Education, Mumbai, Head of the Department, AEHM Division for providing necessary facilities to conduct the research work. Authors also express sincere gratitude to the Department of Science and Technology, Govt. of India for providing funds under project No. DST/TMD-EWO WTI/2K19/EWFH/2019/214". Authors also acknowledge the support provided by Dr. Vidya Shree Bharti for providing facility for preparation of biochar.

CONFLICT OF INTEREST

The author declares no conflict of interest.

AUTHORS' CONTRIBUTION

Tapas Paul: Writing – original draft & Investigation. Rishika M S: Writing reviewing & editing, Bhautik D. Savaliya: Writing – review & editing. Saurav Kumar: Investigation, Conceptualization. Pritam Sarkar: Writing – review & editing, Prasenjit Pal: Data Curation, S.P. Shukla, Kundan Kumar, Ashish Kumar Jha: Supervision, Ganesh Kumar: Writing – review & editing, Supratim Malla: Writing – review & editing.

DATA AVAILABILITY STATEMENT

The data that support the findings of this study are available on a reasonable request from the corresponding author.

REFERENCES

Ahmed MB, Zhou JL, Ngo HH, Johir MAH, Sun L, ... Belhaj D (2018) Sorption of hydrophobic organic contaminants on functionalized biochar: protagonist role of π-π electron-donor-acceptor interactions and hydrogen bonds. Journal of Hazardous Materials 360: 270–278.

Amin FR, Huang Y, He Y, Zhang R, Liu G, Chen C (2016) Biochar applications and modern techniques for characterization. Clean Technologies and Environmental Policy 18(5): 1457–1473.

Box GE, Behnken DW (1960) Some new three level designs for the study of quantitative variables. Technometrics 2(4): 455–475.

Brausch JM, Rand GM (2011) A review of personal care products in the aquatic environment: environmental concentrations and toxicity. Chemosphere 82(11): 1518–1532.

Celcey Z (2019) The embryotoxicity of some phenol derivatives on zebrafish, *Danio rerio*. Caspian Journal of Environmental Sciences 17(1): 11–22.

Chatterjee N, Sinha D, Lemma-Dechassa M, Tan S, Shogren-Knaak MA, Bartholomew B (2011) Histone H3 tail acetylation modulates ATP-dependent remodeling through multiple mechanisms. Nucleic Acids Research 39(19): 8378–8391.

Chen H, Yang X, Wang H, Sarkar B, Shaheen SM, ... Rinklebe J (2020) Animal carcass-and wood-derived biochars improved nutrient bioavailability, enzyme activity, and plant growth in metal-phthalic acid ester co-contaminated soils: a trial for reclamation and improvement of degraded soils. Journal of Environmental Management 261: 110246.

Chiron S, Minero C, Vione D (2007) Occurrence of 2, 4-dichlorophenol and of 2, 4-dichloro-6-nitrophenol in the Rhône river delta (Southern France). Environmental Science & Technology 41(9): 3127–3133.

Czech B, Kończak M, Rakowska M, Oleszczuk P (2021) Engineered biochars from organic wastes for the adsorption of diclofenac, naproxen and triclosan from water systems. Journal of Cleaner Production 288: 125686.

Dong W, Xing J, Chen Q, Huang Y, Wu M, ... Xing B (2024) Hydrogen bonds between the oxygen-containing functional groups of biochar and organic contaminants significantly enhance sorption affinity. Chemical Engineering Journal 499: 156654.

Ensley HE, Barber JT, Polito MA, Oliver AI (1994) Toxicity and metabolism of 2, 4-dichlorophenol by the aquatic angiosperm *Lemna gibba*. Environmental Toxicology and Chemistry 13(2): 325–331.

Freundlich HMFZ (1906) Stoechiometrie und Verwandtschaftslehre. Zeitschriftfuer Physikalische Chemie 57: 385–470 (in German).

Ghosh SK (2016) Biomass & bio-waste supply chain sustainability for bio-energy and bio-fuel production. Procedia Environmental Sciences 31: 31–39.

Gopinath KP, Vo DVN, Gnana Prakash D, Adithya Joseph A, Viswanathan S, Arun J (2021) Environmental applications of carbon-based materials: a review. Environmental Chemistry Letters 19(1): 557–582.

Hall RA, Hara M, Knoll W (1996) Isomerization and acid–base behavior in polyion complex langmuir–blodgett films. Langmuir 12(10): 2551–2555.

Ho YS, Ng JCY, McKay G (2000) Kinetics of pollutant sorption by biosorbents. Separation and Purification Methods 29(2): 189–232.

Hu Y, Li D, Ma X, Liu R, Qi Y, ... Huang D (2021) Effects of 2, 4-dichlorophenol exposure on zebrafish: implications for the sex hormone synthesis. Aquatic Toxicology 236: 105868.

Imade O, Ilesanmi BV, Ogunwole GO, Elekofehinti OO, Souza MCO, ... Adeyemi JA (2024) Effects of 2, 4-

dichlorophenol on non–specific immunity, histopathological lesions, and redox balance in African catfish, *Clarias gariepinus* (Burchell, 1822). Journal of Toxicology and Environmental Health, Part A 87(11): 480–495.

Kumar G, Kumar S, Paul T, Pal P, Shukla SP, ... Pradeep S (2024a) Ecotoxicological risk assessment of triclosan, an emerging pollutant in a riverine and estuarine ecosystems: a comparative study. Marine Pollution Bulletin 205: 116667.

Kumar K, Sarkar P, Paul T, Shukla SP, Kumar S (2024b) Ecotoxicological effects of triclosan on *Lemna minor*: bioconcentration, growth inhibition and oxidative stress. Environmental Science and Pollution Research 31(45): 56550–56564.

Langmuir I (1918) The adsorption of gases on plane surfaces of glass, mica and platinum. Journal of the American Chemical Society 40(9): 1361–1403.

Latch DE, Packer JL, Stender BL, VanOverbeke J, Arnold WA, McNeill K (2005) Aqueous photochemistry of triclosan: formation of 2, 4-dichlorophenol, 2, 8-dichlorodibenzo-p-dioxin, and oligomerization products. Environmental Toxicology and Chemistry 24(3): 517–525.

Li Q, Yu J, Chen W, Ma X, Li G, ... Deng J (2018) Degradation of triclosan by chlorine dioxide: reaction mechanism, 2, 4-dichlorophenol accumulation and toxicity evaluation. Chemosphere 207: 449–456.

Li Y, Li Q, Wu C, Luo X, Yu X, Chen M (2020) The inappropriate application of the regression Langmuir Qm for adsorption capacity comparison. Science of the Total Environment 699: 134222.

Liu S, Ma Y, Liu H, Wang S (2025) The adsorption–desorption behavior of 2, 4-dichlorophenol on microplastics in waters with different salinity. International Journal of Environmental Science and Technology 22(4): 2565–2576.

Matolia J, Shukla SP, Kumar S, Kumar K, Singh AR (2019) Physical entrapment of chitosan in fixed-down-flow column bed enhances triclosan removal from water. Water Science and Technology 80(7): 1374–1383.

Mohammadi A, Sandberg M, Venkatesh G, Eskandari S, Dalgaard T, ... Granström K (2019) Environmental analysis of producing biochar and energy recovery from pulp and paper mill biosludge. Journal of Industrial Ecology 23(5): 1039–1051.

Moussavi G, Khosravi R (2011) The removal of cationic dyes from aqueous solutions by adsorption onto pistachio hull waste. Chemical Engineering Research and Design 89(10): 2182–2189.

Pan X, Wei J, Zou M, Chen J, Qu R, Wang Z (2021) Products distribution and contribution of (de) chlorination, hydroxylation and coupling reactions to 2, 4-dichlorophenol removal in seven oxidation systems. Water Research 194: 116916.

Petroutsos D, Katapodis P, Samiotaki M, Panayotou G, Kekos D (2008) Detoxification of 2, 4-dichlorophenol by the marine microalga *Tetraselmis marina*. Phytochemistry 69(3): 707–714.

Ponnuchamy M, Kapoor A, Jacob MM, Awasthi A, Mukhopadhyay M, ... Prabhakar S (2025) Adsorptive removal of endocrine disruptor bisphenol A from aqueous environment using sugarcane bagasse derived biochar. Journal of the Taiwan Institute of Chemical Engineers 166: 105216.

Prasannamedha G, Kumar PS, Shivaani S, Kokila M (2022) Sodium alginate/magnetic hydrogel microspheres from sugarcane bagasse for removal of sulfamethoxazole from sewage water: batch and column modeling. Environmental Pollution 307: 119523.

Rishika MS, Kumar S, Paul T, Shukla SP, Bharti VS, Kumar K (2024) Performance evaluation of sugarcane bagasse biochar based fixed bed column for removal of triclosan from aqueous solution in presence of humic acid: mechanism, kinetics and safety. Journal of Water Process Engineering 64: 105672.

Sharma P, Sharma S, Sharma SK, Jain A, Shrivastava K (2024) Review on recent advancement of adsorption potential of sugarcane bagasse biochar in wastewater treatment. Chemical Engineering Research and Design 206: 428–439.

Song B, Gong J, Tang W, Zeng G, Chen M, ... Yang Y (2020) Influence of multi-walled carbon nanotubes on the microbial biomass, enzyme activity, and bacterial community structure in 2, 4-dichlorophenol-contaminated sediment. Science of the Total Environment 713: 136645.

Sun K, Kang F, Waigi MG, Gao Y, Huang Q (2017) Laccase-mediated transformation of triclosan in aqueous solution with metal cations and humic acid. Environmental Pollution 220: 105–111.

Tahir H, Sultan M, Akhtar N, Hameed U, Abid T (2016) Application of natural and modified sugar cane bagasse for the removal of dye from aqueous solution. Journal of Saudi Chemical Society 20: S115–S121.

Tan XF, Zhu SS, Wang RP, Chen YD, Show PL... Ho SH (2021) Role of biochar surface characteristics in the adsorption of aromatic compounds: Pore structure and functional groups. Chinese Chemical Letters 32(10): 2939–2946.

Thomas HC (1944) Heterogeneous ion exchange in a flowing system. Journal of the American Chemical Society 66(10): 1664–1666.

Tran HN, Bollinger JC, Lima EC, Juang RS (2023) How to avoid mistakes in treating adsorption isotherm data (liquid and solid phases): Some comments about correctly using Radke-Prausnitz nonlinear model and Langmuir equilibrium constant. Journal of Environmental Management, 325, p.116475

Wahyudi DP, Ghaisani SV, Bismo S (2020) Degradation of

2, 4-dichlorophenol in aqueous solution by ozonation in the presence of iron oxide compound in bubble column reactor. Engineering Journal 24(4): 183–193.

Weber Jr WJ, Morris JC (1963) Kinetics of adsorption on carbon from solution. Journal of the Sanitary Engineering Division 89(2): 31–59.

Wu P, Ata-Ul-Karim ST, Singh BP, Wang H, Wu T, ... Chen W (2019) A scientometric review of biochar research in the past 20 years (1998–2018). Biochar 1(1): 23–43.

Xia X, Hua C, Xue S, Shi B, Gui G, ... Guo L (2016) Response of selenium-dependent glutathione peroxidase in the freshwater bivalve *Anodonta woodiana* exposed to 2, 4-dichlorophenol, 2, 4, 6-trichlorophenol and pentachlorophenol. Fish & Shellfish Immunology 55: 499–509.

Yoon YH, Nelson JH (1984) Application of gas adsorption kinetics I. A theoretical model for respirator cartridge service life. American Industrial Hygiene Association Journal 45(8): 509–516.

Zafeer MK, Menezes RA, Venkatachalam H, Bhat KS (2024) Sugarcane bagasse-based biochar and its potential applications: a review. Emergent Materials 7(1): 133–161.